0090-9556/10/3801-122–132$20.00
DRUG METABOLISM AND DISPOSITION
Vol. 38, No. 1
28688/3540943
DMD 38:122–132, 2010
Printed in U.S.A.

Quantifying the Metabolic Activation of Nevirapine in Patients by Integrated Applications of NMR and Mass Spectrometries[S]

Abhishek Srivastava, Lu-Yun Lian, James L. Maggs, Masautso Chaponda, Munir Pirmohamed, Dominic P. Williams, and B. Kevin Park

MRC Centre for Drug Safety Science, Department of Pharmacology and Therapeutics, School of Biomedical Sciences (A.S., J.L.M., M.C., M.P., D.P.W., B.K.P.) and NMR Centre for Structural Biology (L.-Y.L.), School of Biological Sciences, the University of Liverpool, Liverpool, United Kingdom

Received June 1, 2009; accepted September 29, 2009

ABSTRACT:

Nevirapine (NVP), an antiretroviral drug, is associated with idiosyncratic hepatotoxicity and skin reactions. Metabolic pathways of haptenation and immunotoxicity mechanisms have been proposed. NVP is metabolized by liver microsomes to a reactive intermediate that binds irreversibly to protein and forms a GSH adduct. However, no reactive metabolite of NVP, trapped as stable thioether conjugates, has hitherto been identified in vivo. This study has defined the metabolism of NVP with respect to reactive intermediate formation in patients and a rat model of NVP-induced skin reactions. An integrated NMR and mass spectrometry approach has been developed to discover and quantify stable urinary metabolite biomarkers indicative of NVP bioactivation in patients. Two isomeric NVP mercapturates were identified in the urine of HIV-positive patients undergoing standard antiretroviral chemotherapy. The same conjugates were found in rat bile and urine. The mercapturates were isolated from rat bile and characterized definitively by NMR as thioethers substituted at the C-3 and exocyclic C-12 positions of the methylpyrido ring of NVP. It is proposed that NVP undergoes bioactivation to arene oxide and quinone methide intermediates. The purified major mercapturate was quantified by NMR and used to calibrate a mass spectrometric assay of the corresponding metabolite in patient urine. This is the first evidence for metabolic activation of NVP in humans, and only the second minimum estimate in patients of bioactivation of a widely prescribed drug associated with idiosyncratic toxicities. The method can be used as a template for comparative estimations of bioactivation of any drug in patients.

This study was supported in part by the Wellcome Trust [Grant GR078857MA] (clinical recruitment); the MRC Centre for Drug Safety Science; and the Leche Trust and World Friendship Fund (to A.S).

Parts of this work were presented as follows: Maggs JL, Pirmohamed M, Park BK, and Williams DP (2007) Metabolic activation of nevirapine in human and rat systems. *British Pharmacological Society Winter Meeting 2007*; 2007 Dec 17–20; Brighton, Sussex, UK. British Pharmacological Society, London, UK; Srivastava A, Williams DP, Maggs JL, Lian LY, Gardner I, Chaponda M, Pirmohamed M, and Park BK (2008) Bioactivation of nevirapine: characterization and quantification of nevirapine mercapturate in human urine. *British Pharmacological Society Winter Meeting 2008*; 2008 Dec 16–19; Brighton, Sussex, UK. British Pharmacological Society, London, UK.

M.C. is a Wellcome Trust Clinical Training Fellow.

Article, publication date, and citation information can be found at http://dmd.aspetjournals.org.

doi:10.1124/dmd.109.028688.

[S] The online version of this article (available at http://dmd.aspetjournals.org) contains supplemental material.

Nevirapine [(NVP) Viramune; Boehringer Ingelheim UK, Bracknell, Berkshire, UK] (Fig. 1) is a non-nucleoside reverse transcriptase inhibitor that is widely used for the treatment of HIV infections in the developing world. NVP is associated with two serious clinically restrictive side effects: skin reactions and hepatotoxicity (Patel et al., 2004). Although these may occur simultaneously (Claes et al., 2004), cutaneous hypersensitivity can develop in the absence of liver toxicity and vice versa. Increases of liver enzymes in serum during therapy with NVP are not uncommon but are usually mild to moderate. However, severe, life-threatening, and, in some rare cases, fatal hepatotoxicity has been reported in both HIV-infected patients (Buyse et al., 2006) and non–HIV-infected individuals (Patel et al., 2004) taking NVP. For this reason, NVP has been given a black box warning for hepatotoxicity by the Food and Drug Administration.

Although the role of an immune-mediated mechanism in the skin rash and hepatotoxicity has been advocated strongly (Popovic et al., 2006), it is not yet clear whether this induction of the immune system is caused by a (reactive) metabolite or NVP itself. Indirect clinical

ABBREVIATIONS: NVP, nevirapine; NAC, *N*-acetylcysteine; OH NVP, hydroxynevirapine; 4-carboxy NVP, 4-carboxynevirapine; BN, Brown Norway; P450, cytochrome P450; HLM, human liver microsomes; RLM, rat liver microsomes; LC/MS/MS, liquid chromatography/tandem mass spectrometry; HPLC, high-performance liquid chromatography; LC/MS, liquid chromatography/mass spectrometry; MRM, multiple reaction monitoring; NVP-M1, minor nevirapine mercapturate; SPE, solid-phase extraction; NVP-G2, major nevirapine GSH conjugate; NVP-M2, major nevirapine mercapturate; DQFCOSY, double quantum-filtered correlation spectroscopy; NOESY, nuclear Overhauser enhancement spectroscopy; APAP, acetaminophen; amu, atomic mass unit; NVP-G1, minor nevirapine GSH conjugate; 2D, two-dimensional; NOE, nuclear Overhauser effect; 1D, one-dimensional.

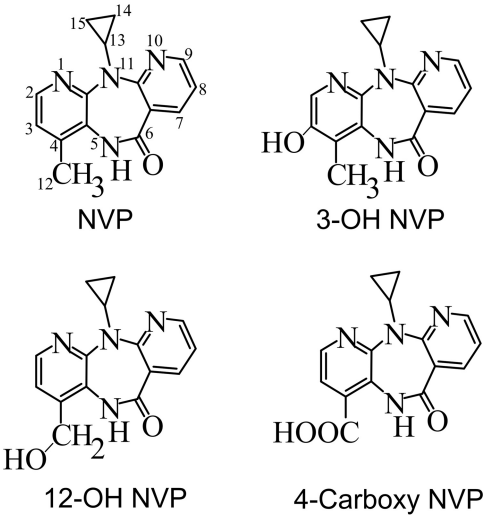

FIG. 1. Chemical structures of NVP, 3-OH NVP, 12-OH NVP, and 4-carboxy NVP.

evidence for drug-induced oxidative damage comes from a case reported by Claes et al. (2004), where a patient with toxic epidermal necrolysis and hepatitis was successfully treated with intravenous human immunoglobulins and *N*-acetylcysteine (NAC).

The stable products of oxidative metabolism of NVP in humans are 2-hydroxynevirapine (2-OH NVP), 3-OH NVP, 8-OH NVP, and 12-OH NVP (Riska et al., 1999a), formed mainly by CYP3A4 and CYP2B6 (Erickson et al., 1999). 12-OH NVP is metabolized to 4-carboxynevirapine (4-carboxy NVP).

Among idiosyncratic, pharmacotherapy-associated skin reactions in humans, those linked with NVP are exceptional because they have been modeled successfully in experimental animals (Popovic et al., 2006). Chen et al. (2008) have proposed that the skin rash produced in Brown Norway (BN) rats by NVP and 12-OH NVP may be caused by NVP quinone methide (Fig. 2) formed through dissociation of 12-OH NVP sulfonate in the skin (Fig. 2). A mild hepatotoxicity, assessed by histopathological and plasma enzyme indicators, is induced in rats pretreated with NVP or dexamethasone (Walubo et al., 2006). This observation implies that one or more NVP metabolites are causal agents of hepatotoxicity, but no mechanistic explanation of the liver injury has emerged. Chen et al. (2008) have suggested that the hepatotoxicity of NVP in humans is caused by quinone methide formed in situ by cytochrome P450 (P450). In addition, a number of antiretroviral drugs inhibit bile acid excretion by hepatocytes—a potential mechanism of hepatotoxicity—but NVP has no effect (McRae et al., 2006).

There may be several pathways for NVP bioactivation (Fig. 2). The cyclopropylamine group has the potential, via *N*-dealkylation, to become bioactivated to an aminium cation radical (Takakusa et al., 2008). 12-OH NVP, a major metabolite in human liver microsomes (HLM), is a substrate for sulfotransferase in rats (Chen et al., 2008), and it has been proposed that the sulfate ester dissociates to form a reactive quinone methide intermediate (Chen et al., 2008). The quinone methide could also be generated, additionally or alternatively, by enzymic oxidation (Wen et al., 2009). Hydroxyheteroaryl metabolites (Riska et al., 1999a) are potential precursors of reactive quinone imines (Wen et al., 2009). Finally, NVP might form one or more heteroarene epoxide intermediates in either of the pyridine rings (Fig. 2). Nevertheless, evidence for metabolic activation of NVP is limited to NADPH-dependent irreversible binding of radiolabeled drug to rat liver microsomes (RLM) (Takakusa et al., 2008), mechanism-based inhibition of microsomal CYP3A4 (Wen et al., 2009), and the metabolism of NVP by HLM and CYP3A4 to a single GSH adduct (Wen et al., 2009).

By developing our early observations of thioether metabolites in rats and patients (Srivastava et al., 2008, 2009), here we have defined the metabolism of NVP with respect to reactive intermediate formation in human patients and in a rat model of NVP-induced skin reactions. An integrated NMR and liquid chromatography/tandem mass spectrometry (LC/MS/MS) approach is described that enabled the discovery and direct quantification of stable urinary metabolite biomarkers that are indicative of NVP bioactivation. Biomarkers such as this can be used to explore associations between metabolic activation and the incidence and risk factors of adverse drug reactions in

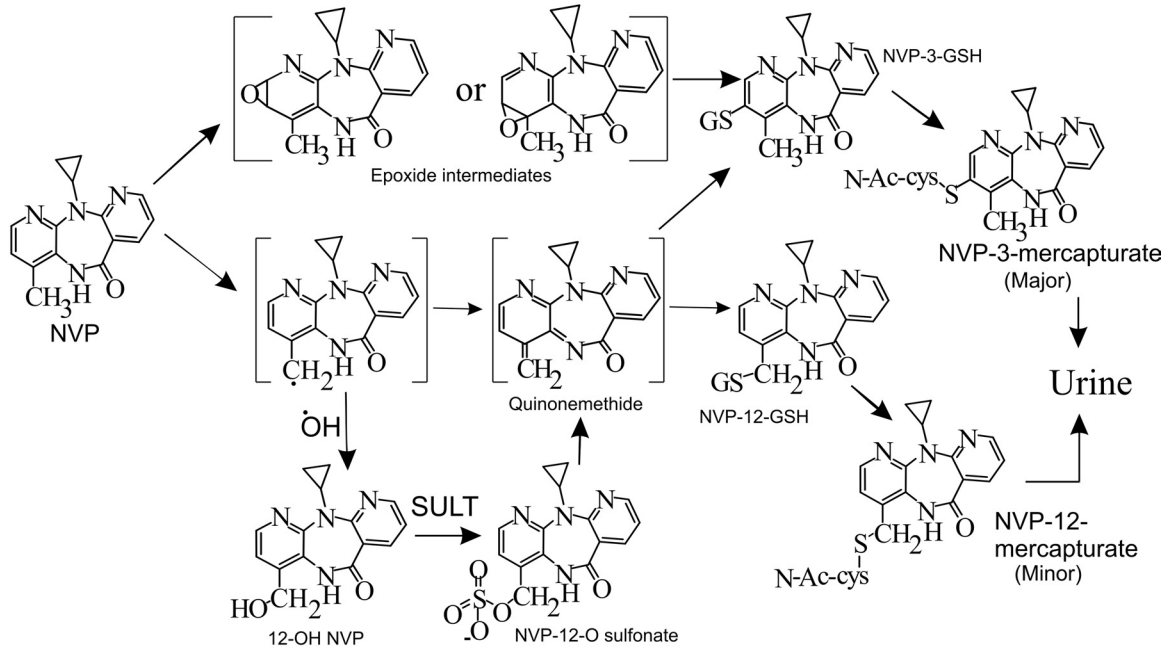

FIG. 2. Proposed scheme for the bioactivation of NVP and possible reactive metabolites.

patients (Gopaul et al., 2003). The strategy developed forms a unique bridge between clinical studies in patients, in vivo animal models, and in vitro cellular studies.

Materials and Methods

Chemicals. NVP (11-cyclopropyl-4-methyl-5*H*-dipyrido[3,2-b:2′,3′-e][1,4] diazepin-6{11*H*}-one), standards of two known metabolites of NVP (3-OH NVP and 12-OH NVP), and descyclopropyl NVP (Fig. 1) were gifts from Pfizer Global Research and Development (Sandwich, Kent, UK). They were 99% pure. NVP tablets (Viramune, 200 mg; Boehringer Ingelheim UK) were purchased from a local pharmacy. GSH, NADPH (tetrasodium salt), NAC, methyl cellulose, Hanks' balanced salt solution, pH 7.4, dimethyl sulfoxide, and tetradeuteromethanol (CD_3OD; 99.8 atom % D) were purchased from Sigma-Aldrich (Poole, Dorset, UK). Methanol, water, and acetonitrile were high-performance liquid chromatography (HPLC) grade from Fisher Scientific UK (Loughborough, Leicestershire, UK). All of the other solvents were of HPLC grade, and unless otherwise specified all of the other reagents were purchased from Sigma-Aldrich.

Extraction of NVP from Tablets. Two Viramune tablets were crushed to a fine powder, and the weight of powder was recorded. To the powder, 200 ml of chloroform was added and shaken vigorously. The mixture was allowed to stand for 1 h. Supernatant was collected, and the solvent evaporated under a stream of nitrogen. The dry residue was crushed to a fine powder and weighed. The content of NVP in this powder (approximately 75–80% w/w) was determined against a standard curve of NVP (1 μM–1 mM) using the analytical HPLC method described below.

All the animal experiments carried out for the isolation of preparative quantities of mercapturates and GSH conjugate for NMR analysis were performed by administering NVP extracted from tablets. The microsomal and hepatocyte incubations and the other animal experiments were carried out using 99% pure NVP.

Experimental Animals. Adult male and female BN rats and adult male Wistar rats were obtained from Charles River Laboratories (Margate, Kent, UK). The protocols described were undertaken in accordance with criteria outlined in a license granted under the Animals (Scientific Procedures) Act 1986 and approved by the University of Liverpool Animal Ethics Committee.

Human Urine. Single-void (spot) urine samples were obtained at unspecified times of day from nine HIV-positive adult patients taking 200 mg of NVP twice daily in Malawi (Fig. 10C). Patients also received stavudine (40 mg twice daily) and lamivudine (150 mg twice daily) as part of anti-HIV combinational chemotherapy. Baseline urine samples were collected immediately before the start of therapy, and drug-containing urine samples were collected 6 weeks after the start of therapy. Ethical approval was obtained from the College of Medicine Research Ethics Committee, Blantyre, Malawi, and the Liverpool School of Tropical Medicine Research Ethics Committee. All the patients gave informed consent.

Rat Bile. The male Wistar (350–450 g; $n = 6$) and the male (150–250 g; $n = 3$) and female (150–250 g; $n = 3$) BN rats were terminally anesthetized with urethane (140 mg/kg, isotonic saline, i.p.) and cannulated via trachea, jugular vein, and common bile duct. NVP (150 mg/kg; 2 ml/kg dimethyl sulfoxide) was administered intravenously. Bile was collected for 30 min before administration of NVP and thereafter hourly for 5 to 7 h. 12-OH-NVP (75 mg/kg; 2 ml/kg dimethyl sulfoxide) was also administered intravenously to three cannulated male Wistar rats. Additional male Wistar rats ($n = 3$) were predosed with dexamethasone (100 mg/kg, corn oil, i.p.) 24 h before administration of NVP.

Rat Urine. NVP (0.5 or 1 g/kg) suspended in 0.5% methyl cellulose (75 mg/ml) was dosed orally to adult male Wistar rats (200–300 g; $n = 3$) and female BN rats (150–180 g; $n = 3$) in two equal doses at an interval of 6 h. Rats were kept in metabolism cages, and their urine was collected for 24 h after the first dose. Control rats were dosed with the vehicle.

Solid-Phase Extraction. Human urine (5–10 ml), rat urine (5–10 ml), and rat bile (1–4 ml) were concentrated using methanol/water-preconditioned Waters (Manchester, UK) Sep-Pak classic C18 cartridges (360 mg, 55–105 μm). Loaded cartridges were washed with distilled water, and the crude extract was eluted with methanol (4 ml). The eluate was evaporated under nitrogen at 50°C, and the dry residue reconstituted in 50% methanol (0.3–1 ml).

Rat Hepatocytes. Hepatocytes were isolated from adult male Wistar rats (200–300 g; $n = 4$) using a two-step collagenase perfusion method (Graham et al., 2008), and cell viability was assessed by trypan blue exclusion. In general, viability was 85 to 95%. Hepatocytes were only used when viability was greater than 75%. NVP (50 μM) added as methanol solution (final methanol content, 0.5% v/v) was incubated with the hepatocytes (2×10^6/ml; $n = 3$ incubations) in a final volume of 6 ml of HEPES incubation buffer (Graham et al., 2008) for 0 to 4 h. Incubations were carried out at 37°C in an orbital shaker set at 190 rpm. Drug was omitted from the control incubations. After 4 h of incubation, 6 ml of acetonitrile was added to stop the reaction. The mixture was centrifuged at 870*g* for 10 min. The supernatant was removed and evaporated under nitrogen. The dry residue was reconstituted in 300 μl of 50% methanol and kept at −20°C until analysis.

HLM and RLM. HLM and RLM were prepared by a differential ultracentrifugation method (Graham et al., 2008). Approximately 10-g samples of human livers that had been obtained from two male (aged 24 and 41 years) and two female (aged 10 and 36 years) renal transplant donors and stored at −80°C were used for the preparation of microsomes. Ethical approval for the study was granted, and consent for removal of the liver samples was obtained from the donors' relatives. RLM were prepared from whole livers of adult male Wistar rats (200–300 g). Incubations ($n = 3$ replicates) were carried out in a final volume of 1 ml of Hanks' balanced salt solution, pH 7.4, containing 1 or 3 mg/ml microsomal protein and 10 or 25 μM NVP added as a methanol solution (final methanol content, 0.5% v/v). The reactions were initiated by the addition of NADPH (final concentration, 1 mM; omitted from control incubations) and performed by incubation for 1 h in a shaking water bath at 37°C. To assess the ability of the microsomes to bioactivate NVP, by trapping the reactive intermediates, some incubations also contained either GSH or NAC (1 or 2 mM). The microsomal reaction was terminated by the addition of an equal volume of ice-cold acetonitrile. After overnight precipitation of the protein at −20°C, the incubations were centrifuged at 870*g* for 10 min. The supernatant was evaporated to dryness under nitrogen. It was reconstituted in 300 μl of 50% methanol and left at −20°C until analysis.

Analytical HPLC. The metabolites of NVP were resolved with a Hypersil BDS C18 column (25 × 0.46 cm, 5-μm particle size; Thermo Fisher Scientific, Runcorn, Cheshire, UK). The mobile phase consisted of a combination of acetonitrile containing formic acid (0.05%, v/v) and 15 mM ammonium formate buffer (adjusted to pH 4 with formic acid). A sample aliquot of 50 μl was injected onto the column and eluted at 1 ml/min with a gradient of 5 to 17% acetonitrile over 10 min, maintaining 17% acetonitrile for 25 min, and finally reverting to 5% acetonitrile over 5 min. The analytes were detected at 240 nm.

Preparative HPLC for NVP Mercapturates. The method used to obtain the preparative quantities of pure NVP mercapturates used a Columbus C18 column (250 × 4.6 cm, 5-μm particle size; Phenomenex, Macclesfield, Cheshire, UK). Mobile phase consisted of acetonitrile (containing 0.05% formic acid) and water (containing 0.07% formic acid) with a gradient of 10 to 20% acetonitrile over 5 min, maintaining 20% acetonitrile for 20 min, and finally reverting to 10% acetonitrile over 5 min. The collection of metabolites was performed at room temperature. Flow rate and sample volume were 1.0 ml/min and 50 μl, respectively. All of the separations were monitored at 240 nm.

Preparative HPLC for NVP GSH Conjugates. A Supelcosil LC-CN column (250 × 4.6 cm, 5-μm particle size; Supelco, Bellefonte, PA) was used with mobile phase consisting of acetonitrile (containing 0.05% formic acid) and water (containing 0.07% formic acid). An aliquot of 50 μl was injected onto the column and eluted at 1 ml/min with a gradient of 2 to 25% acetonitrile over 35 min. The analytes were detected at 240 nm. The collection of metabolite was performed at room temperature.

Liquid Chromatography/Mass Spectrometry and LC/MS/MS Analyses. A Quattro II mass spectrometer (Waters) fitted with the standard coaxial electrospray source was used for liquid chromatography/mass spectrometry (LC/MS) in the positive-ion mode. The LC system consisted of two Jasco PU980 pumps (Jasco UK, Great Dunmow, Essex, UK) and a Jasco HG-980-30 mixing module. Analytes were resolved on a Hypersil BDS C18 column (Thermo Fisher Scientific) according to the method described above. Eluate split-flow to the LC/MS interface was approximately 50 μl/min. Nitrogen was used as the nebulizing and drying gas. The interface temperature was 80°C,

and the capillary voltage was 3.9 kV. Spectra were acquired between *m/z* 100 and 1050 over a scan duration of 5 s. In-source fragmentation of analyte ions was achieved at a cone voltage of 70 V. Data were processed with MassLynx 3.5 software (Waters).

LC/MS/MS analyses were performed using an Applied Biosystems/MDS Sciex (Foster City, CA) API 2000 mass spectrometer with TurboIonSpray source. Analytes were resolved on a Hypersil BDS C18 column (Thermo Fisher Scientific) according to the method described above. Eluate split-flow to the LC/MS interface was approximately 200 μl/min. Nitrogen was used as collision gas. NVP and metabolites were detected in the multiple-reaction monitoring (MRM) mode with the following transitions: NVP, *m/z* 267 to *m/z* 226; NVP mercapturates, *m/z* 428.3 to *m/z* 299; NVP GSH conjugates, *m/z* 572 to *m/z* 443 and *m/z* 572 to *m/z* 299. Data were acquired and processed with the Analyst Software (version 1.4; Applied Biosystems/MDS Sciex). The main working parameters for MRM and product ion scanning are given in Supplemental Table 1.

Isolation and Purification of Minor NVP Mercapturate. To obtain preparative quantities of the minor mercapturate (NVP-M1), two adult male Wistar rats (500–600 g) received a single intraperitoneal injection of dexamethasone (100 mg/kg; 4 ml/kg corn oil) and after 24 h were given an oral dose of NVP (800 mg/kg; 4 ml/kg 0.5% w/v methyl cellulose). Approximately 10 ml of bile was collected in 5 to 7 h. Bile was concentrated by solid-phase extraction (SPE) and reconstituted with 1 ml of 50% methanol. The retention time of NVP-M1 was established through comparisons of UV (240 nm) and mass chromatograms of pre- and postdosing bile. Aliquots of bile (50 μl) were chromatographed by the analytical HPLC method, and the fraction of eluate between 15 and 17 min was collected. The fractions obtained from 20 runs were combined, evaporated under a nitrogen stream, and reconstituted with 500 μl of 50% methanol. The reconstituted material was used to purify NVP-M1 by the preparative HPLC method (eluate fraction 15–16 min). All of the collected fractions were combined and evaporated under a nitrogen stream at 50°C. The dry residue was stored at −20°C for NMR analysis.

Isolation and Purification of Major NVP Mercapturate and GSH Conjugate from Rat Bile. To obtain preparative quantities of the major GSH conjugate (NVP-G2) and major mercapturate (NVP-M2), two adult male Wistar rats (500–600 g) were administered a larger oral dose of NVP (600–800 mg/kg), and bile was collected according to the method described above. Bile (10 ml) was concentrated by SPE and reconstituted with 1 ml of 50% methanol. The initial isolation of the NVP-G2 and NVP-M2 was achieved by the analytical HPLC method that used a Hypersil BDS C18 column (Thermo Fisher Scientific). For this experiment, 50-μl aliquots of bile were chromatographed, and the fractions of eluate between 12 and 14.5 min (for NVP-G2) and 16 and 18 min (for NVP-M2) were collected. The fractions obtained from 20 runs were combined, dried under a nitrogen stream, and reconstituted with 500 μl of 50% methanol. The reconstituted fractions were used to purify the NVP-G2 (eluate fraction 22–23 min) and NVP-M2 (eluate fraction 18–19 min) by the preparative HPLC methods described above.

Characterization of NVP Mercapturates and GSH Conjugate by NMR. The purified mercapturates were dissolved in tetradeuteromethanol, and all the spectra were acquired nonspinning at 288K. Total sample volumes were approximately 600 μl in 5-mm NMR tubes (final concentrations, approximately 14–17 μg/ml NVP-M1, 34–42 μg/ml NVP-M2, and 14–17 μg/ml NVP-G2). Chemical shifts are reported in parts per million with the shift of methanol referenced to 3.31 ppm. The ^{1}H spectra were acquired with eight scans, using a spectral width of 11 ppm and 32×10^3 data points in the time domain. The free induction decays were zero-filled to 64×10^3 points and multiplied by an exponential window function with the line-broadening parameter set at 0.5 Hz. The double quantum-filtered correlation spectroscopy (DQFCOSY) and nuclear Overhauser enhancement spectroscopy (NOESY) spectra were acquired in phase-sensitive modes with 4096 points and a spectral width of 11 ppm in both the F1 and F2 dimensions. The DQFCOSY spectra were acquired using a relaxation delay of 1.8 s, 164 transients, and 512 increments. The NOESY spectra were acquired using parameters similar to these and a mixing time of 1 s. The free induction decays were processed (zero-filled in F1 to 2048 points) using shifted sine-bell squared window functions.

NMR Standard Curve and Quantification of NVP-M2. Acetaminophen (APAP) was used to create a standard curve. Each APAP dataset was acquired at a temperature of 288K using a 45° pulse width, 64K data points, 64 scans (with eight dummy scans), and a repetition time of 4.72 s. The receiver gain was optimized automatically using the most concentrated sample to avoid saturation of the receiver. The free induction decays were zero-filled to 256K points and multiplied by an exponential window function with the line-broadening parameter set at 1 Hz. Minimal baseline corrections were required; if these were necessary, they were performed using the standard Bruker (Coventry, UK) routine. A standard curve was prepared by plotting the average integral values of the aromatic protons of APAP against concentration as shown in Fig. 9A. The concentration of the NVP-M2 sample was determined from the integrals of the C2 proton of NVP ring A (Fig. 1) using spectra of the mercapturate acquired under identical spectral parameters and conditions as those of APAP.

Quantification of NVP-M2 in Human Urine. An MRM LC/MS/MS method for the quantification of NVP-M2 and NVP in human urine was developed. Calibration standards of NVP-M2 were prepared using material that had been isolated from rat bile and quantified by ^{1}H NMR spectroscopy. The MRM-calibrated ranges for NVP-M2 (*m/z* 428.3/299) and NVP (*m/z* 267/226) were 0.062 to 2 μM and 0.078 to 5 μM, respectively. Analytes were resolved on a Hypersil BDS C18 column (Thermo Fisher Scientific) according to the method described above, and the main operating parameters for MRM are given in Supplemental Table 1. Before the analysis, urine samples (50 μl) were mixed with acetonitrile (1:1, v/v), and the mixtures were centrifuged at 18,400*g* for 5 min. Aliquots of supernatant (50 μl) were taken for LC/MS/MS analysis.

Results

Urinary Metabolites of NVP in Humans. NVP, identified by coelution with an authentic standard, and eight metabolites (M1–M8) in human urine were resolved by HPLC (Fig. 3A). The metabolites were located initially by comparing the UV chromatograms (240 nm) of pre- and postdosing urine. None of these metabolites, or any of the metabolites found elsewhere in this study, corresponded to the authentic standard of descyclopropyl NVP. In LC/MS analysis (Fig. 3B), the most polar metabolites (M1, M2, and M3), at low cone voltages (≤30 V), gave peaks at *m/z* 459 that were assigned to $[M + 1]^+$ of *O*-glucuronides of monooxygenated NVP from the indicative neutral loss of dehydroglucuronic acid (*m/z* 283, $[M + 1–176]^+$) (Fig. 3B). M5 exhibited an ion at *m/z* 297, corresponding to $[M + 1]^+$ of the carboxylic acid metabolite of NVP (Fig. 3B). This metabolite has been identified previously by Riska et al. (1999a,b) as the 4-carboxy NVP. M4, M6, and M8 were identified as hydroxy metabolites of NVP with $[M + 1]^+$ at *m/z* 283. M6 and M8 were characterized as 12- and 3-OH NVP, respectively, by coelution with authentic standards, but M4 could not be characterized. Primary alcohol M6 underwent diagnostic facile dehydration ($[M + 1\text{-}H_2O]^+$). M7 produced a weak ion at *m/z* 428 (Fig. 3B) that can be assigned to $[M + 1]^+$ of a mercapturate of NVP. At a higher cone voltage (70 V) this metabolite was found to produce a major fragment at *m/z* 299, which corresponds to the characteristic neutral loss of *N*-acetyldehydroalanine [129 atomic mass units (amu)] from a mercapturate (Scholz et al., 2005).

Urinary and Biliary Metabolites of NVP in Rats. Urine samples from female BN and male Wistar rats and bile samples from male and female BN and male Wistar rats were analyzed by HPLC and LC/MS. The use of BN and Wistar rats allowed comparisons of NVP's metabolites in strains that, respectively, have and have not been associated with an adverse skin reaction to NVP. None of these analyses found qualitative differences between metabolite profiles that could be associated with either strain or sex. In both urine and bile, NVP was found to be metabolized to three glucuronide conjugates of monooxygenated NVP (M1, M2, and M3) (Fig. 3, C and D) with $[M + 1]^+$ at *m/z* 459, carboxy metabolite M5 (4-carboxy NVP, *m/z* 297, $[M + 1]^+$), three hydroxy NVP metabolites (M4, M6/12-OH, and M8/3-OH; *m/z* 283, $[M + 1]^+$), and one metabolite (M9)

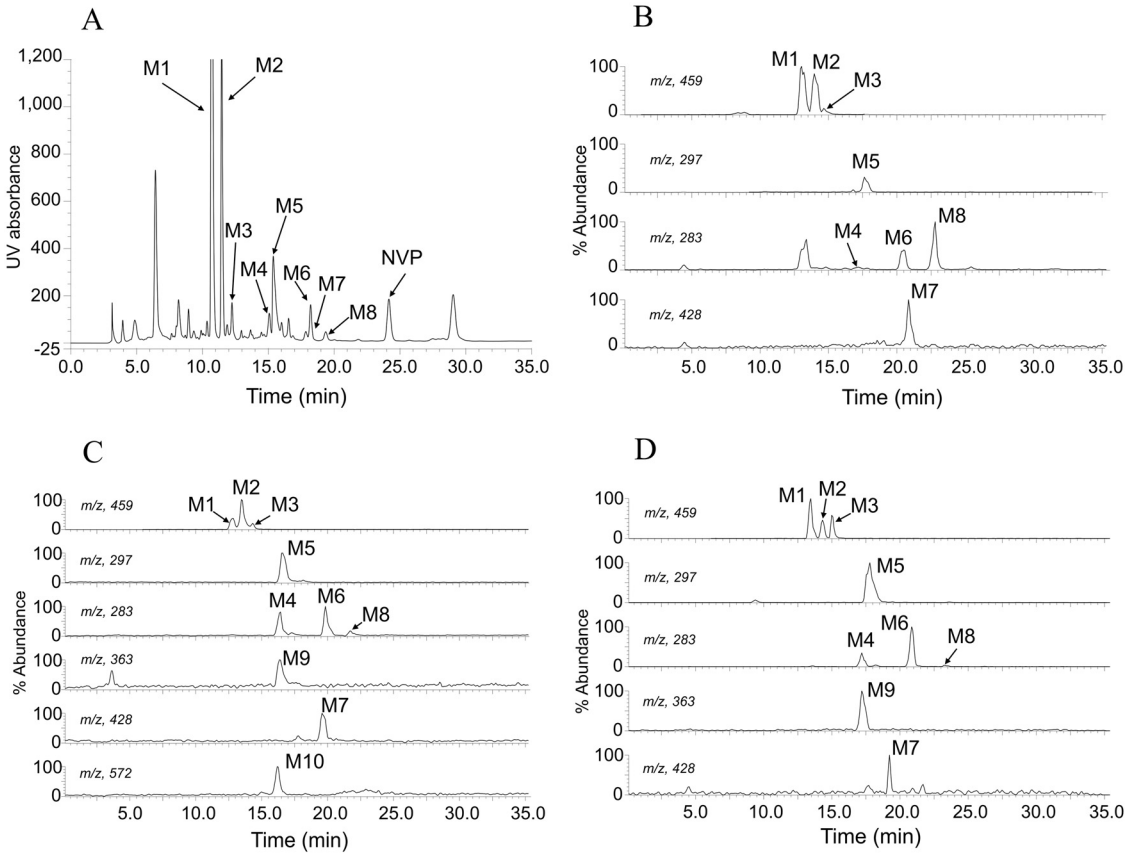

FIG. 3. Analysis of NVP metabolites in humans and rats. A, HPLC-UV chromatogram of the metabolites of NVP in patient's urine. LC/MS ion current chromatograms of NVP metabolites in patient's urine (B), rat bile (C), and rat urine (D). The structural assignments of peaks M1 through M10 are given in Table 1.

identified as a sulfonate conjugate of hydroxy NVP (Fig. 3, C and D). In positive-ion scan, M9 exhibited an ion at *m/z* 363 ($[M + 1]^+$) and in negative-ion mode yielded a strong peak at *m/z* 361. It was shown to be derived from 12-OH NVP as the bile samples obtained after administering 12-OH NVP to male Wistar rats contained a coeluting peak in the mass chromatogram for *m/z* 363. Rat bile and urine also contained a mercapturate conjugate (*m/z* 428, $[M + 1]^+$) (Fig. 3, C and D) that coeluted with the human mercapturate (M7) and yielded the same major fragment at *m/z* 299 ($[M + 1–129]^+$). In addition, a GSH conjugate of NVP was found in rat bile (M10). The mass chromatogram for *m/z* 572 ($[M + 1]^+$) contained one major peak (Fig. 3C). The metabolite's product ion spectrum obtained by LC/MS/MS included ions indicative of the generic neutral loss of a γ-glutamyl moiety (*m/z* 443, $[M + 1–129]^+$) and fragmentation at a thioether linkage ($[M + 1–273]^+$) (data not shown).

Metabolism of NVP by Rat Hepatocytes. By LC/MS analysis, primary hepatocytes from male Wistar rats were found to produce three glucuronide conjugates (M1, M2, and M3) and the three hydroxy NVP metabolites (M4, 12-OH, and 3-OH). One mercapturate

TABLE 1

Metabolites of NVP in rat and human systems

The MRM transitions (bold) were used to detect the corresponding thioether metabolites.

	$[M + 1]^+$ or MRM Transition	NVP Metabolite	Human Urine	HLM	Rat Bile	Rat Urine	Rat Heps	RLM
	m/z							
M1	459	OH-NVP-glucuronide*	√	X	√	√	√	X
M2	459	OH-NVP-glucuronide*	√	X	√	√	√	X
M3	459	OH-NVP-glucuronide*	√	X	√	√	√	X
M4	283	OH-NVP*	√	√	√	√	√	√
M5	297	4-Carboxy NVP	√	X	√	√	√	X
M6	283	12-OH NVP	√	√	√	√	√	√
M7 (NVP-M2)	428, **MRM, 428.3 → 299**	NVP-3-mercapturate	√	√	√	√	√	√
M8	283	3-OH NVP	√	√	√	√	√	√
M9	363	NVP-12-sulfonate†	X	X	√	√	X	X
M10 (NVP-G2)	572, **MRM, 572 → 443**	NVP-3-GSH	X	√	√	X	√	√
NVP-M1	428, **MRM, 428 → 299**	NVP-12-mercapturate	√	X	√	√	√	X
NVP-G1	572, **MRM, 572 → 443**	NVP-12-GSH‡	X	X	√	X	√	X

√, Present; X, not detected by LC/MS/MS; Heps, hepatocytes.
* Position of substituent was not characterized.
† Position of substituent was not characterized but could be inferred from metabolism of 12-OH NVP.
‡ Position of substituent was not characterized but could be inferred by analogy with the formation of two NVP mercapturates.

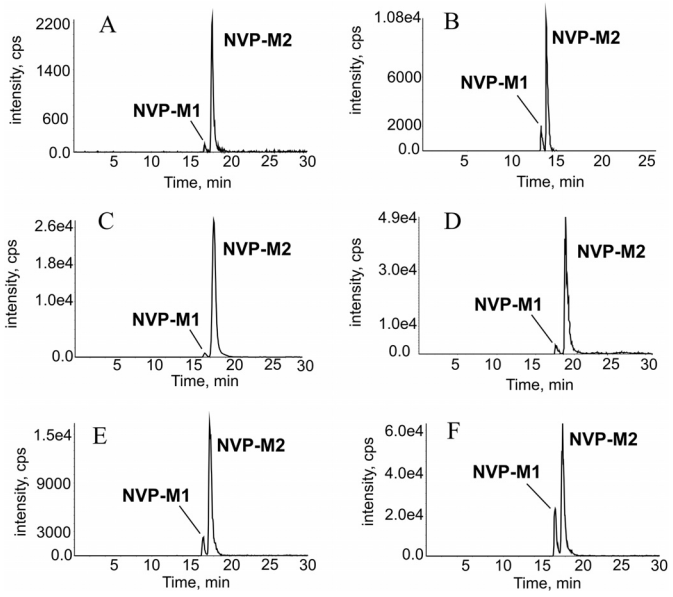

FIG. 4. Identification of NVP mercapturates. LC/MS/MS transition from *m/z* 428.3 to *m/z* 299 demonstrating the presence of two NVP mercapturates (NVP-M1 and NVP-M2) in human urine (A), urine of female BN rat (B), bile of female BN rat (C), bile of male BN rat (D), bile of uninduced male Wistar rat (E), bile of dexamethasone-induced male Wistar rat (F). The transition was monitored after injection of 50 μl of pooled human urine (from nine HIV-positive patients), rat bile, or urine.

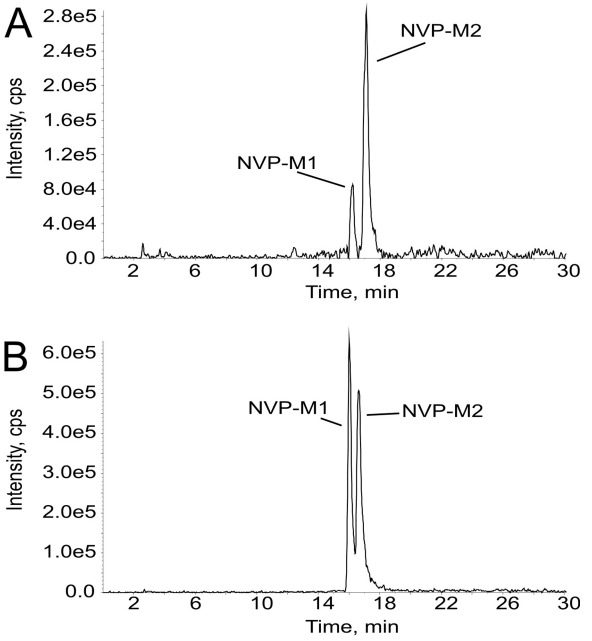

FIG. 5. LC/MS ion current (*m/z* 428) chromatograms of mercapturate conjugates of NVP in the bile (100-μl aliquots) of uninduced Wistar rat (A) and dexamethasone-induced Wistar rat (B). The relative amounts of NVP-M1 and NVP-M2 eliminated in bile of uninduced (1:7) and dexamethasone-induced (1:1) rats were estimated from the corresponding chromatographic peak areas.

(M7), one GSH conjugate (M10), and one carboxy NVP metabolite (M5) were also found in rat hepatocytes (Table 1).

Metabolism of NVP by HLM and RLM. NVP underwent metabolism in HLM and microsomes from male Wistar rats to form three hydroxy NVP metabolites (M4, M6/12-OH, and M8/3-OH). As before, M6 and M8 were assigned to 12- and 3-OH NVP, respectively, by coelution with authentic standards. These assignments were corroborated by the selective dehydration of primary alcohol 12-OH NVP ($[M + 1\text{-}H_2O]^+$) during electrospray ionization. Although M4 could not be identified, comparisons with the findings of Erickson et al. (1999), who obtained 2-, 3-, 8-, and 12-OH NVP in HLM, and the chromatograms of Riska et al. (1999a,b) suggest it was probably 2-OH NVP. Those incubations supplemented with GSH and NAC formed one GSH conjugate (M10) and one mercapturate (M7), respectively (Table 1), and these conjugates were absent from control incubations.

In Vivo Screening for Stable Metabolite Biomarkers of NVP Bioactivation in Humans and Rats. After the observation of mercapturate (M7) and GSH conjugate (M10) by LC/MS analysis (Fig. 3), human and rat urine and rat bile were screened by LC/MS/MS (MRM) for the presence of any additional NVP mercapturate(s) (*m/z* 428, $[M + 1]^+$) and GSH conjugate(s) (*m/z* 572, $[M + 1]^+$).

The MRM (NVP mercapturates, *m/z* 428.3 to *m/z* 299; NVP GSH conjugates, *m/z* 572 to *m/z* 443 and *m/z* 572 to *m/z* 299) survey found two NVP mercapturates (NVP-M1 and NVP-M2) in human urine (Fig. 4A). Bile and urine obtained from female BN rats (the animal model for NVP-induced skin rash) (Chen et al., 2008), bile (dexamethasone-induced and noninduced) and urine from male Wistar rats, and bile from male BN rats also contained these mercapturates (Fig. 4). In addition, two analogous GSH conjugates (NVP-G1 and NVP-G2) were observed in rat bile (data not shown). However, and notwithstanding the extensive alkyl and aryl hydroxylation of NVP (Erickson et al., 1999; Riska et al., 1999a,b; Chen et al., 2008), no GSH adduct or mercapturate of mono-/dioxygenated NVP was found in any of the bile or urine samples. The major thioether metabolites, NVP-M2 and NVP-G2, corresponded chromatographically and mass spectrometrically to M7 and M10, respectively, namely, the metabolites found in the preliminary LC/MS analyses. The minor thioether metabolites, NVP-M1 and NVP-G1, were only detected by LC/MS/MS screening. In human urine and bile from noninduced Wistar rats, NVP-M2, from a comparison of parent-ion peak areas, was consistently 5- to 10-fold more abundant than NVP-M1. Using the same method of comparison, the induction of P450 in male Wistar rats ($n = 3$) by dexamethasone resulted in an approximately 5- to 10-fold increase in the concentration of NVP-M1 in bile as that compared with the noninduced rats, but there was only a 1.5- to 2-fold increase in the concentration of NVP-M2 (Fig. 5). This result indicates that dexamethasone selectively increases the turnover of NVP to NVP-M1, suggesting that different P450s in male rats catalyze the formation of the electrophilic precursors of NVP-G1 and NVP-G2. The major GSH conjugate's peak in the Q1 scan for *m/z* 572 was 10 to 30 times more abundant than the corresponding peak for the minor GSH conjugate, whereas the ratio of the major to minor coeliminated mercapturate was 5 to 10.

In Vitro Screening for Stable Metabolite Biomarkers of NVP Bioactivation in Humans and Rats. Rat hepatocytes produced two NVP mercapturates coeluting with the human urine and rat bile mercapturates (NVP-M1 and NVP-M2). The two analogous GSH conjugates (NVP-G1 and NVP-G2) were also observed. HLM and RLM produced a mercapturate coeluting with NVP-M2 and a GSH conjugate coeluting with NVP-G2 (data not shown). However, in contrast to human and rat urine, rat bile, and rat hepatocytes, NVP-M1 and NVP-G1 were not found in microsomal incubations.

Confirmation of Chemical Identities of Human and Rat Mercapturates. The product ion spectra of NVP-M1 and NVP-M2 in human urine and bile of male Wistar rats (dexamethasone-induced and noninduced) and in bile of female BN rats (Fig. 6) were analyzed to confirm chemical identity across species. The fragment ions of *m/z* 428.3 obtained from either NVP-M1 or NVP-M2 were the same for the rat and human metabolites. However, whereas NVP-M1 yielded abundant ions at *m/z* 265, 251, 238, 224, and 196, NVP-M2 yielded its most abundant ions at *m/z* 299, 258, 214, 161, and 140 (Fig. 6).

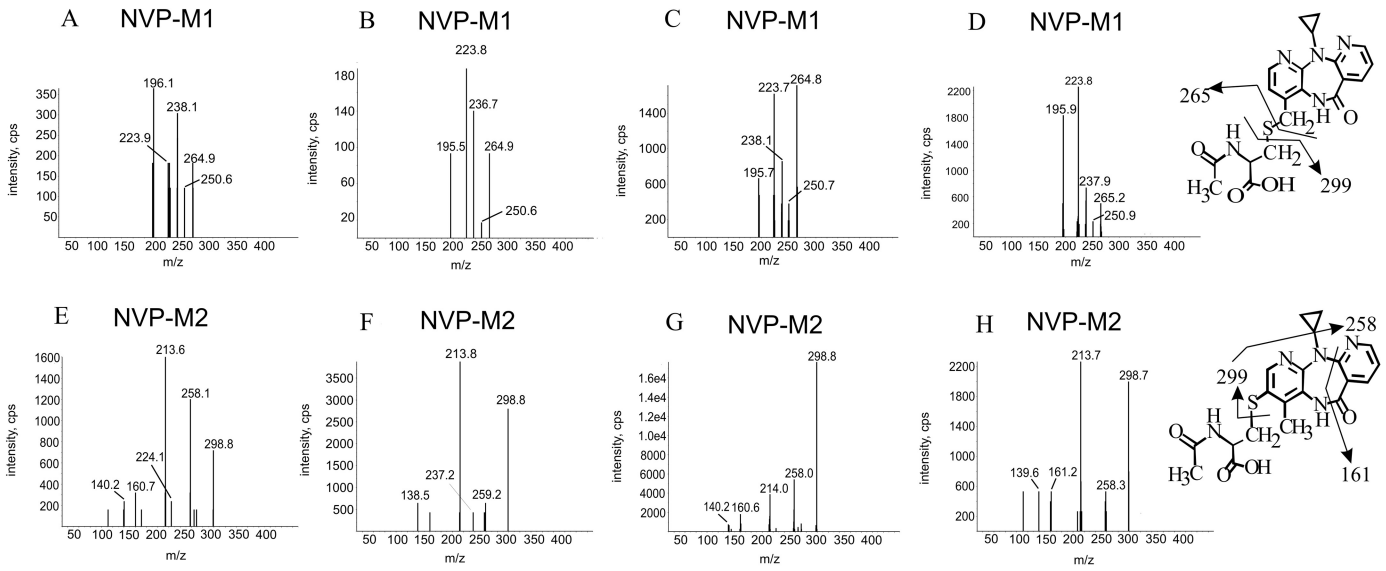

FIG. 6. Confirmation of chemical similarity of NVP mercapturates across humans and rats. Representative product ion spectra of the $[M + 1]^+$ (*m/z* 428) of NVP mercapturates excreted in human urine and rat bile. Pooled patients' urine (10 ml) was concentrated 10-fold by SPE, and 150 μl was analyzed to obtain the spectra of mercapturates NVP-M1 (A) and NVP-M2 (E). B and F are the spectra obtained from mercapturates in female BN rat bile. C and G are the spectra obtained from mercapturates in Wistar rat bile. D and H are the spectra obtained from mercapturates in bile of dexamethasone-induced Wistar rat.

Although *m/z* 299 did not appear in the centroided spectrum of NVP-M1, it was observable in the profile data.

Isolation and Purification of NVP Mercapturates and GSH Conjugate from Rat Bile. Bile collected from rats administered large doses of NVP was found to be an abundant source of NVP-M2 and NVP-G2, but NVP-M1 was produced in amounts sufficient for isolation and chemical characterization by NMR spectroscopy only after P450 induction with dexamethasone. Rat urine was not a useful source of NVP mercapturates because it contained closely eluting, endogenous, UV-absorbing components that significantly impeded the metabolites' purification. Production of NVP-G1 was also enhanced by dexamethasone, but it was not possible to isolate material that was sufficiently pure for characterization by NMR. The induction of NVP's bioactivation in rats by dexamethasone, and hence the enhanced production of thioether metabolites, was predicted from the observation of Chen et al. (2008) that NVP undergoes covalent binding to CYP3A when it is metabolized by the expressed rat enzyme. Subsequently, Wen et al. (2009) showed that NVP is metabolized to a GSH adduct by CYP3A4. Dexamethasone is a highly effective inducer of hepatic CYP3A1 in male Wistar rats and also induces CYP3A2 (Kishida et al., 2008). In addition, 2- and 12-hydroxylations of NVP catalyzed by CYP3A isoforms, as represented by human CYP3A4 and CYP3A5 (Erickson et al., 1999), are potentially bioactivation pathways through the generation of reactive epoxide and quinone methide intermediates (Chen et al., 2008), respectively.

A multistep HPLC/UV approach using consecutively the analytical and preparative HPLC methods yielded approximately 8 to 10 μg and 20 to 25 μg of pure NVP-M1 (Supplemental Fig. 1) and NVP-M2 (Supplemental Fig. 2), respectively (values estimated from a standard curve prepared with NVP). However, only one GSH conjugate (NVP-G2) was purified successfully (approximately 12–15 μg) (Supplemental Fig. 2).

Characterization of NVP Mercapturates by NMR. The ^{1}H NMR spectra of the purified NVP-M1 (Fig. 7) and NVP-M2 (Fig. 8A) are shown with the expanded aromatic region plotted above each of the complete spectra. Spectral assignment of NVP-M2 was unexpectedly complicated because, at 15°C, it adopted two conformations, which were apparent from doubling of some of the proton and carbon

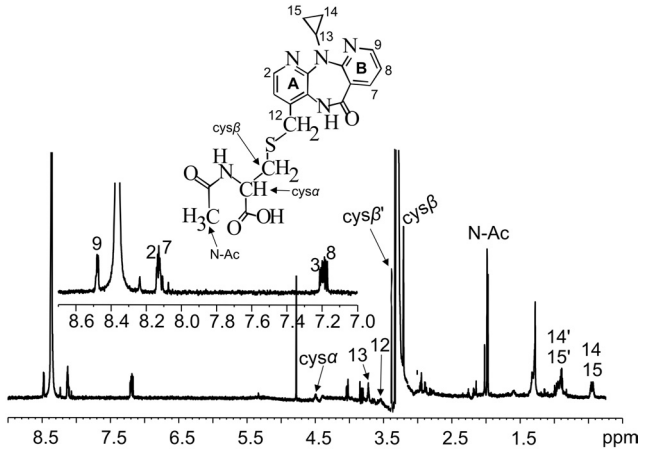

FIG. 7. Structural characterization of NVP-M1. Shown is one-dimensional (1D) ^{1}H NMR spectrum of NVP-M1 isolated and purified from dexamethasone-induced Wistar rat bile. Expanded aromatic region is shown above the spectrum.

resonances. This conformational heterogeneity was absent at temperatures greater than 30°C. All of the following results refer to the spectra acquired at 15°C.

The DQFCOSY spectrum of NVP-M2 at 288K is shown in Fig. 8, D and E (full spectrum and expanded region). Two types of spin systems are discerned. The proton at 8.337 ppm (conformation 1) and at 8.324 ppm (conformation 2) is a singlet (Fig. 8E). The resonances at 8.475, 8.096, and 7.2 ppm form a coupled spin system: the protons at 8.475 and 8.096 ppm are a doublet of doublets, whereas the proton at 7.2 ppm is a triplet (Fig. 8A). These resonances must be from ring B of the NVP moiety. This was confirmed by comparing the DQFCOSY spectrum of NVP-M2 with that of the NVP. These data show that the NAC moiety is conjugated to NVP via ring A.

The two-dimensional (2D) NOESY spectrum established that the NAC moiety is bound to the C3 position of NVP-M2 for the following reasons. Molecular models of NVP (Fig. 8, B and C) suggest that a substitution at C3 would give rise to a nuclear Overhauser effect (NOE) between the C4-CH_3 (12) of NVP and the S-CH_2 (cys-β) protons of the NAC moiety (Fig. 8F). In addition, the NOE was

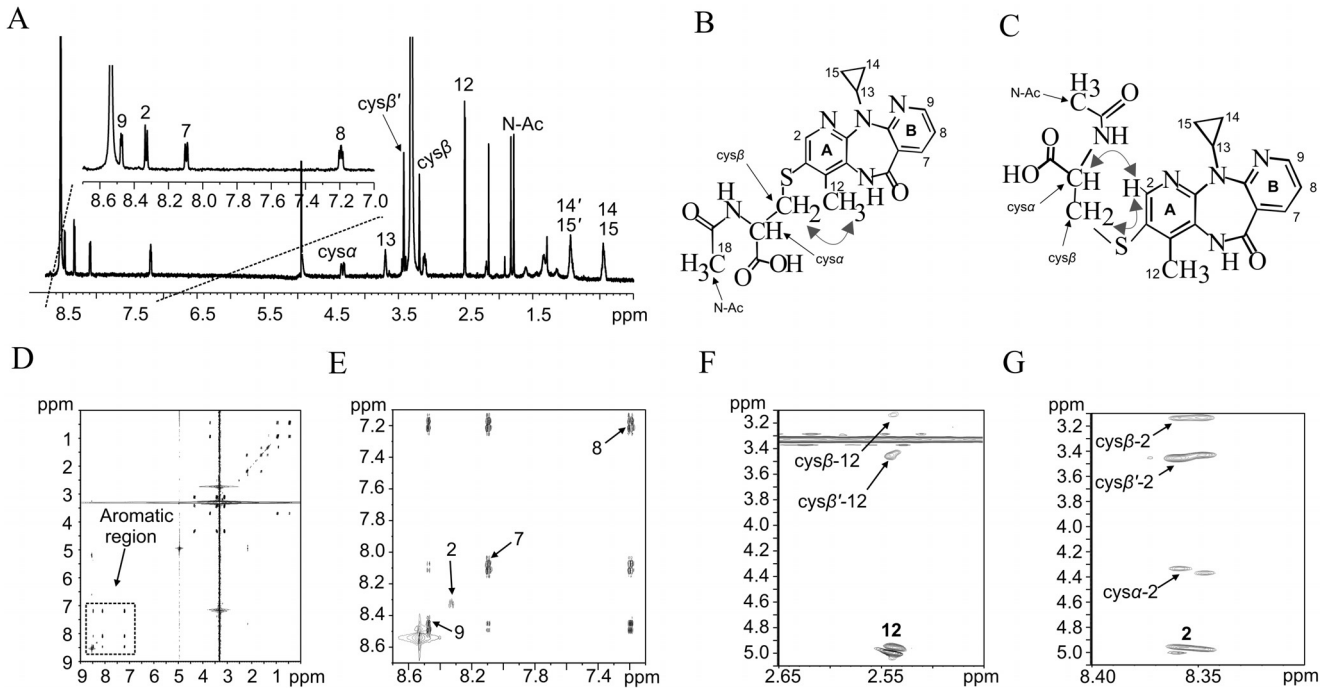

FIG. 8. Structural characterization of NVP-M2. A, representative 1D ^{1}H NMR spectrum of NVP-M2 isolated and purified from Wistar rat bile. Expanded aromatic region is shown above the spectrum. B and C, represent the structure of NVP-M2 in different conformations as elucidated by chemical modeling. The conformationally significant NOEs are highlighted by arrows. D, 2D DQFCOSY spectrum of NVP-M2. E, expanded 2D DQFCOSY spectrum between 7 and 8.8 ppm. F and G represent 2D NOESY spectra of NVP-M2; NOE between different protons are shown by arrows.

observed between the C2 proton of NVP and the methylene (cys-β) and methine (cys-α) protons of the S-CH_2-CH group (Fig. 8G). These NOE data confirm that C3 is the position of thioether conjugation on ring A. The structure of the NVP conjugate is shown (Fig. 8, B and C), with the conformationally significant NOE highlighted.

As mentioned earlier, the conformational heterogeneity of NVP-M2 is deduced from the doubling of some proton resonances; most obvious are the resonances from the *N*-acetyl CH_3 and the C(2)H of ring A. From the chemical model it would appear that rotation about the C3-S bond gives rise to these multiple conformations at 15°C.

The aromatic region of the ^{1}H NMR spectrum of NVP-M1 revealed spin systems consistent with the compound shown in Fig. 7. The resonances at 8.48 (doublet), 8.11 (doublet), and 7.19 (doublet of doublet) ppm form a coupled spin system similar to ring B of NVP-M2. The resonances at 7.21 and 8.14 ppm are coupled to each other and are assigned, respectively, to C(2)H and C(3)H of ring A. An NOE cross-peak is observed between C(3)H and the C(12) methylene protons, confirming that NVP is substituted at the exocyclic C(12) position. This is further supported by the disappearance from the spectrum of NVP-M1 of the singlet resonance at 2.63 ppm, which is assigned to the C(12)H3 in the major mercapturate.

Characterization of NVP-G2 by NMR. The ^{1}H NMR spectrum of the purified NVP-G2 is shown (Fig. 9A) with the expanded aromatic region plotted above the spectrum. The sections of the NOESY spectrum of the GSH conjugate are shown in Fig. 9C. The NOESY spectrum of NVP-G2] (Fig. 9C) had similar singlet and coupled spin systems as the NVP-M2 spectrum (Fig. 8G). NOE cross-peaks are also detected between the C2 proton of NVP and the methylene (cys-β) and methine (cys-α) protons of the S-CH_2-CH group of the cysteine residue (Fig. 9C). The structure of the NVP GSH conjugate is shown (Fig. 9B) with the conformationally significant NOE highlighted. Using interpretations similar to those applied to the spectra of the NVP-M2, the data indicate that the GSH moiety is attached to ring A at the C3 position.

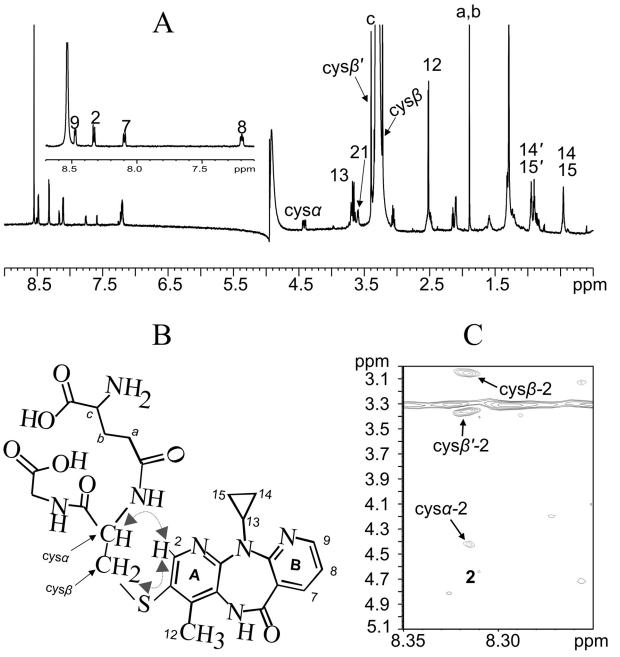

FIG. 9. Structural characterization of NVP-G2. A, representative 1D ^{1}H NMR spectrum of NVP-G2 isolated and purified from Wistar rat bile. Expanded aromatic region is shown above the spectrum. B, the structure of NVP-G2 (NVP-3-GSH conjugate) with conformationally significant NOE highlighted. C, 2D NOESY spectrum of NVP-G2; NOE between different protons are shown by arrows.

Quantification of NVP-M2 in Human Urine Samples. The absolute mass of the purified NVP-M2 determined by the NMR method using an APAP standard curve (Fig. 10A) was 21 μg. This standardized sample was used to calibrate the LC/MS/MS method (Fig. 10B), and thereby to quantify the NVP-M2 in spot urine

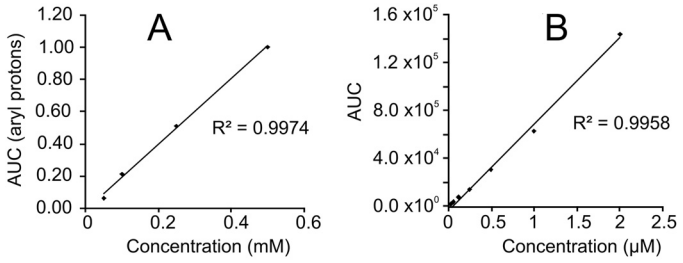

C

Patient No	Age	Sex	NVP_M2 (μg/ml)	NVP (μg/ml)	$\frac{\text{NVP-M2}}{\text{NVP}} X10^2$
1	36	Male	0.03	7.79	0.43
2	46	Male	0.13	10.20	1.32
3	46	Male	0.15	8.83	1.72
4	45	Male	0.17	5.97	2.81
5	38	Male	0.17	8.23	2.06
6	42	Male	0.22	11.29	1.97
7	28	Male	0.61	19.86	3.09
8	47	Female	0.69	11.46	6.03
9	42	Female	0.74	9.01	8.19

FIG. 10. Quantification of NVP-M2 in human urine. A, NMR standard curve of APAP. B, LC/MS/MS standard curve of NVP-M2. C, table showing the levels of NVP-M2 and unmetabolized NVP in patients' urine samples.

samples from nine patients (Fig. 10C). The lowest concentration of NVP-M2 was 0.03 μg/ml, and the highest was 0.7 μg/ml. The urinary metabolite ratio (NVP-M2/NVP $\times$ 100) was 0.43 to 8.19; mean, 3.07 (Fig. 10C).

The specificity of the LC/MS/MS assays was shown by analyzing drug-free urine samples and determining that no isobaric endogenous or environmental constituents coeluted with either NVP or NVP-M2. The absence of analytical interference from the known coadministered drugs, namely, stavudine or lamivudine, and from lamivudine *S*-oxide (the only metabolite of either drug reported to be an abundant urinary metabolite), was shown by analyzing drug-containing urine samples and establishing that both target analytes were clearly resolved from these compounds (ΔR_t 6–7 min before NVP-M2), none of which was isobaric with either NVP or NVP-M2 ($\Delta m/z \leq 21$ below NVP).

Discussion

It is thought that many severe adverse drug reactions arise as a consequence of drug bioactivation (Park et al., 2005). Therefore, the detection of chemically reactive metabolites early in drug discovery and safety assessment is a major concern (Uetrecht, 2003). However, the role of bioactivation in idiosyncratic toxicity remains controversial. A major problem for risk assessment has been the lack of bioanalytical tools that can be used for characterization of bioactivation in in vitro screens and also in patients and animal models of drug toxicity. Therefore, we have developed an integrated bioanalytical strategy for the characterization and quantification of stable biomarkers of drug bioactivation, using NVP as a paradigm, providing a bridge between clinical studies in patients, in vivo animal models, and in vitro cellular studies (Fig. 11).

We have shown that NVP is bioactivated in patients and in a rat model of NVP-induced cutaneous hypersensitivity reactions (Chen et al., 2008) by characterizing novel NVP mercapturates, potentially formed from multiple reactive metabolites. The mercapturates and GSH conjugates of NVP were found in the context of numerous oxygenated and/or conjugated (glucuronidated and sulfonated) metabolites that have been identified in earlier studies (Riska et al., 1999a,b). However, the patients' urinary NVP mercapturates held the greatest interest because metabolites of this type have been recognized

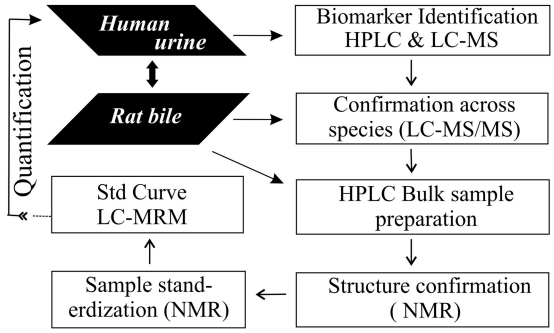

FIG. 11. Flow chart representing the integrated NMR and LC/MS/MS approach for the discovery and quantification of stable urinary metabolite biomarkers indicative of NVP bioactivation.

for many years as particularly useful biomarkers in assessments of human exposure to chemically diverse environmental and biogenic electrophiles (Seutter-Berlage et al., 1977). Mercapturates are associated generically with tissue exposure to low molecular weight electrophilic precursors of GSH adducts (Hinchman and Ballatori, 1994). On the other hand, GSH conjugates are unsuitable biomarkers of metabolic activation in vivo because they are only very rarely eliminated in urine and seemingly only at very low concentrations (Johnson and Plumb, 2005). They have been found as *N*-acetylated derivatives (Tsuruda et al., 1995).

The LC/MS/MS method used here for detection of mercapturates used a neutral loss of 129 amu (*N*-acetyldehydroalanine) in positive-ion mode. Neutral loss of 129 amu from parent anions is generally regarded as the generic fragmentation of mercapturates (Scholz et al., 2005), and thereby, as a β-elimination reaction, is obtained irrespective of the type of thioether linkage, i.e., (hetero) aryl, cycloalkyl, alkylaryl, and alkyl. Jian et al. (2009) have developed LC/MS/MS screens for mercapturates based on the negative-ion neutral loss of 129 amu or MRM involving this loss as survey scans that trigger the acquisition of fragment-rich, positive-ion, product ion spectra. However, the NVP mercapturates did not yield ions in negative-ion analysis and presumably would not be found by screens of this type. The primary structural insight was provided by the product ion spectra of the mercapturates (Fig. 6) and was derived from a difference between scissions of the thioether linkage. Whereas the prominent fragment at *m/z* 299 in the product ion spectrum of NVP-M2 corresponds to the characteristic β-elimination of *N*-acetyldehydroalanine (129 amu), NVP-M1 yielded an ion at *m/z* 265 that is attributed to neutral loss of NAC (163 amu) (Scholz et al., 2005). This retro-Michael elimination might be expected to be more favorable for an alky-linked thioether rather than an (hetero)aryl-linked thioether.

The substitution positions of the NVP mercapturates found in human urine and in rat urine and bile were definitively characterized by NMR as NVP C-12 (NVP-M1) and NVP C-3 (NVP-M2) (Figs. 7 and 8). It can be concluded that NVP undergoes bioactivation in vivo through the involvement of C-3 and C-12 (Fig. 2). However, the C-3 position is more favorable for oxidation and/or nucleophilic attack as 5 to 10 times higher levels of NVP-M2 were observed in rat bile by LC/MS analysis (Fig. 5A). We have also identified two GSH conjugates in rat bile, but only the major, NVP-G2, conjugate (NVP-G2/NVP-G1, 10–30) was characterized by NMR, as the thioether substituted at C-3 (Fig. 9). By analogy with the two mercapturates, NVP-G1 can be identified inferentially as NVP-12-GSH.

The NVP 3-mercapturate is likely to be derived from the unhindered 2,3-epoxide or possibly from the hindered 3,4-epoxide (Fig. 2). 2-OH-NVP and 3-OH-NVP are both putative products of rearrangement of the 2,3-epoxide and are metabolites of NVP (Erickson et al.,

1999). In a recent study, Chen et al. (2008) have proposed an alternative or additional route of NVP quinone methide formation in skin, through dissociation of 12-OH NVP sulfonate rather than NVP oxidation (Fig. 2), and raised the possibility that the bioactivation pathways in skin and liver, the major sites of NVP-associated adverse reactions, may differ mechanistically. It is important to note that NVP elicits both hepatotoxicity and serious skin reactions in humans (Patel et al., 2004). Popovic et al. (2006) and Chen et al. (2008) have reported extensively on a rat model of NVP-induced skin rash and concluded that bioactivation is responsible for the toxicity. However, this rat model does not show any evidence of hepatotoxicity. We have addressed, metabolically, the similarity between this model and patients, and linked them through the formation of two mercapturates as common metabolites, but the mercapturates are not necessarily derived from a common product of bioactivation.

Until now, the only substantive evidence for metabolic activation of NVP in vivo was the observation by Takakusa et al. (2008) that the ^{14}C-labeled drug undergoes irreversible binding to liver tissue and plasma protein in rats. Although [^{14}C]NVP was subject to NADPH-dependent irreversible binding to RLM, it did not undergo NADPH-dependent binding to HLM (Takakusa et al., 2008). NVP can modify CYP3A4 covalently as a mechanism-based inhibitor and is metabolized to a GSH adduct by HLM and CYP3A4 (Wen et al., 2009). Wen et al. (2009) have deduced that this adduct is formed by addition of GSH to either the benzylic carbon or an aryl position of the quinone methide intermediate (Fig. 2) first proposed by Chen et al. (2008). However, as only one mercapturate and GSH adduct [NVP-3-mercapturate (NVP-M2) and NVP-3-GSH (NVP-G2), respectively] was formed by HLM (Table 1), either the purely oxidative reactions of unsupplemented HLM fail to reproduce metabolic activation of NVP in vivo or HLM do not trap the reactive metabolite(s) with GSH or NAC via both the addition reactions that operate in vivo. A coincubation of HLM and GSH or a GSH derivative is now a standard preparation used in screens for reactive metabolites that are soft electrophiles (Gan et al., 2009), but it frequently yields more conjugates than can be accounted for in vivo (Bu et al., 2007; Rousu et al., 2009). NVP is an exception and emphasizes the need for whole animal studies. Production of the second GSH adduct in vivo may be ascribed to a selective dependence on conjugation catalyzed by cytosolic GSH transferase. Alternatively, it may be in part an extrahepatic process. Any NVP mercapturate produced extrahepatically could be eliminated in bile, as rat liver possesses an efficient mechanism for uptake and biliary excretion of circulating mercapturates (Hinchman et al., 1998). Both adducts might derive from the quinone methide (Fig. 2) as GSH does not always react exclusively at the benzylic carbon of methide intermediates (Fan and Bolton, 2001; Wang et al., 2009). However, the selectively increased proportion of NVP-M1 in bile of dexamethasone-induced rats indicates the intrahepatic formation of at least two oxidized precursors of NVP GSH adducts in this species.

The reactive intermediate(s) might augment the depletion of hepatic GSH in HIV-positive patients with chronic hepatitis infection that is linked to their HIV-positive status (Barbaro et al., 1996). This additional depletion of GSH, if it is uncompensated, may exacerbate the oxidative stress associated with viral hepatitis and AIDS (Stehbens, 2004), consequently initiating secondary hepatocellular damage of greater severity. The rapid remediation of NVP-associated toxic epidermal necrolysis and hepatitis in a patient treated with, among other things, NAC (Claes et al., 2004), a precursor of GSH, suggests restoration of GSH levels might have aided recovery in this case. Moreover, enhanced haptenation of tissue proteins by reactive NVP metabolites under the circumstances of depleted GSH might also lead to the initiation of an immune response.

We have quantified the major NVP mercapturate (NVP-M2) excreted in patient urine by a LC/MS/MS assay (Fig. 10). The only other examples of this type of analysis for human pharmaceuticals are those of paracetamol, phenacetin, felbamate, and valproic acid, where the drug mercapturates were identified and quantified (Siegers et al., 1984; Veronese et al., 1985; Thompson et al., 1999; Dieckhaus et al., 2002; Gopaul et al., 2003). However, this is only the second minimum estimate in humans of bioactivation of an idiosyncratically toxic drug that is still used widely. The toxicity of paracetamol and phenacetin is regarded as essentially dose-dependent. Metabolic activation of felbamate, an antiepileptic drug associated with idiosyncratic aplastic anemia and hepatotoxicity, can also be assessed in patients by monitoring (two) urinary mercapturates (Dieckhaus et al., 2002). In fact, the urinary metabolite ratio (mercapturate/felbamate $\times$ 100) for the major mercapturate (4.5–27; mean, 14.7) is appreciably higher than it is for NVP-M2 (Thompson et al., 1999). However, the candidate population for felbamate is now highly restricted. Valproic acid, an antiepileptic linked with idiosyncratic clinical hepatotoxicity, is metabolized via a reactive diene to two isomeric urinary mercapturates that are evidence of bioactivation and associated with risk factors for the drug-induced toxicity (Gopaul et al., 2003).

The applicability of NVP mercapturates as clinical biomarkers requires detailed verification, but even at this early stage it should be noted that only a low proportion of mercapturate might be found in urine even if there is extensive bioactivation, if bioactivation coincides with GSH depletion (Dieckhaus et al., 2002). This depletion can occur in HIV-positive patients with chronic hepatitis (Barbaro et al., 1996). Disease state is potentially a significant influence on drug bioactivation: urinary concentrations of the thioether metabolites of paracetamol were significantly higher in AIDS patients than in symptom-free HIV-seropositive subjects (Esteban et al., 1997).

Considerable efforts have been made to develop screening systems for reactive drug metabolites based on subcellular liver fractions (Bauman et al., 2009; Gan et al., 2009) or isolated hepatocytes (Bauman et al., 2009). What is currently lacking is a noninvasive, generic, and quantitative method for assessing bioactivation of drugs in experimental animals, human volunteers, and patients. The integration of NMR and mass spectrometry creates early opportunities for assaying newly characterized metabolites that are of potential biological/toxicological importance but impractical targets for chemical synthesis. Wider availability of powerful spectrometers equipped with cryogenic probeheads is likely to result in increasingly frequent exploitation of NMR to authenticate and quantify complex minor metabolites, which can then be used as reference standards for high-throughput, LC-based, quantitative analyses (Churchill et al., 1986; Espina et al., 2009). The present study can serve as a template for future applications of this method to biomarkers of the metabolic activation of drugs in humans.

Acknowledgments. We thank Dr. Iain Gardner (Pfizer Global R&D, Sandwich, UK) for supplying nevirapine and pure metabolites, and Pfizer Global R&D UK and AstraZeneca (Alderley Park, UK) for equipment.

References

Barbaro G, Di Lorenzo G, Soldini M, Parrotto S, Bellomo G, Belloni G, Grisorio B, and Barbarini G (1996) Hepatic glutathione deficiency in chronic hepatitis C: quantitative evaluation in patients who are HIV positive and HIV negative and correlations with plasmatic and lymphocytic concentrations and with the activity of the liver disease. *Am J Gastroenterol* **91:**2569–2573.

Bauman JN, Kelly JM, Tripathy S, Zhao SX, Lam WW, Kalgutkar AS, and Obach RS (2009) Can in vitro metabolism-dependent covalent binding data distinguish hepatotoxic from non-

hepatotoxic drugs? An analysis using human hepatocytes and liver S-9 fraction. *Chem Res Toxicol* **22:**332–340.
Bu HZ, Zhao P, Dalvie DK, and Pool WF (2007) Identification of primary and sequential bioactivation pathways of carbamazepine in human liver microsomes using liquid chromatography/tandem mass spectrometry. *Rapid Commun Mass Spectrom* **21:**3317–3322.
Buyse S, Vibert E, Sebagh M, Antonini T, Ichai P, Castaing D, Samuel D, and Duclos-Vallée JC (2006) Liver transplantation for fulminant hepatitis related to nevirapine therapy. *Liver Transpl* **12:**1880–1882.
Chen J, Mannargudi BM, Xu L, and Uetrecht J (2008) Demonstration of the metabolic pathway responsible for nevirapine-induced skin rash. *Chem Res Toxicol* **21:**1862–1870.
Churchill FC, Mount DL, Patchen LC, and Björkman A (1986) Isolation, characterization and standardization of a major metabolite of amodiaquine by chromatographic and spectroscopic methods. *J Chromatogr* **377:**307–318.
Claes P, Wintzen M, Allard S, Simons P, De Coninck A, and Lacor P (2004) Nevirapine-induced toxic epidermal necrolysis and toxic hepatitis treated successfully with a combination of intravenous immunoglobulins and N-acetylcysteine. *Eur J Intern Med* **15:**255–258.
Dieckhaus CM, Thompson CD, Roller SG, and Macdonald TL (2002) Mechanisms of idiosyncratic drug reactions: the case of felbamate. *Chem Biol Interact* **142:**99–117.
Erickson DA, Mather G, Trager WF, Levy RH, and Keirns JJ (1999) Characterization of the in vitro biotransformation of the HIV-1 reverse transcriptase inhibitor nevirapine by human hepatic cytochromes P-450. *Drug Metab Dispos* **27:**1488–1495.
Espina R, Yu L, Wang J, Tong Z, Vashishtha S, Talaat R, Scatina J, and Mutlib A (2009) Nuclear magnetic resonance spectroscopy as a quantitative tool to determine the concentrations of biologically produced metabolites: implications in metabolites in safety testing. *Chem Res Toxicol* **22:**299–310.
Esteban A, Pérez-Mateo M, Boix V, González M, Portilla J, and Mora A (1997) Abnormalities in the metabolism of acetaminophen in patients infected with the human immunodeficiency virus (HIV). *Methods Find Exp Clin Pharmacol* **19:**129–132.
Fan PW and Bolton JL (2001) Bioactivation of tamoxifen to metabolite E quinone methide: reaction with glutathione and DNA. *Drug Metab Dispos* **29:**891–896.
Gan J, Ruan Q, He B, Zhu M, Shyu WC, and Humphreys WG (2009) In vitro screening of 50 highly prescribed drugs for thiol adduct formation–comparison of potential for drug-induced toxicity and extent of adduct formation. *Chem Res Toxicol* **22:**690–698.
Gopaul S, Farrell K, and Abbott F (2003) Effects of age and polytherapy, risk factors of valproic acid (VPA) hepatotoxicity, on the excretion of thiol conjugates of (*E*)-2,4-diene VPA in people with epilepsy taking VPA. *Epilepsia* **44:**322–328.
Graham EE, Walsh RJ, Hirst CM, Maggs JL, Martin S, Wild MJ, Wilson ID, Harding JR, Kenna JG, Peter RM, et al. (2008) Identification of the thiophene ring of methapyrilene as a novel bioactivation-dependent hepatic toxicophore. *J Pharmacol Exp Ther* **326:**657–671.
Hinchman CA and Ballatori N (1994) Glutathione conjugation and conversion to mercapturic acids can occur as an intrahepatic process. *J Toxicol Environ Health* **41:**387–409.
Hinchman CA, Rebbeor JF, and Ballatori N (1998) Efficient hepatic uptake and concentrative biliary excretion of a mercapturic acid. *Am J Physiol* **275:**G612–G619.
Jian W, Yao M, Zhang D, and Zhu M (2009) Rapid detection and characterization of in vitro and urinary N-acetyl-L-cysteine conjugates using quadrupole-linear ion trap mass spectrometry and polarity switching. *Chem Res Toxicol* **22:**1246–1255.
Johnson KA and Plumb R (2005) Investigating the human metabolism of acetaminophen using UPLC and exact mass oa-TOF MS. *J Pharm Biomed Anal* **39:**805–810.
Kishida T, Muto S, Hayashi M, Tsutsui M, Tanaka S, Murakami M, and Kuroda J (2008) Strain differences in hepatic cytochrome P450 1A and 3A expression between Sprague-Dawley and Wistar rats. *J Toxicol Sci* **33:**447–457.
McRae MP, Lowe CM, Tian X, Bourdet DL, Ho RH, Leake BF, Kim RB, Brouwer KL, and Kashuba AD (2006) Ritonavir, saquinavir, and efavirenz, but not nevirapine, inhibit bile acid transport in human and rat hepatocytes. *J Pharmacol Exp Ther* **318:**1068–1075.
Park BK, Kitteringham NR, Maggs JL, Pirmohamed M, and Williams DP (2005) The role of metabolic activation in drug-induced hepatotoxicity. *Annu Rev Pharmacol Toxicol* **45:**177–202.
Patel SM, Johnson S, Belknap SM, Chan J, Sha BE, and Bennett C (2004) Serious adverse cutaneous and hepatic toxicities associated with nevirapine use by non-HIV-infected individuals. *J Acquir Immune Defic Syndr* **35:**120–125.
Popovic M, Caswell JL, Mannargudi B, Shenton JM, and Uetrecht JP (2006) Study of the sequence of events involved in nevirapine-induced skin rash in Brown Norway rats. *Chem Res Toxicol* **19:**1205–1214.
Riska P, Lamson M, MacGregor T, Sabo J, Hattox S, Pav J, and Keirns J (1999a) Disposition and biotransformation of the antiretroviral drug nevirapine in humans. *Drug Metab Dispos* **27:**895–901.
Riska PS, Joseph DP, Dinallo RM, Davidson WC, Keirns JJ, and Hattox SE (1999b) Biotransformation of nevirapine, a non-nucleoside HIV-1 reverse transcriptase inhibitor, in mice, rats, rabbits, dogs, monkeys, and chimpanzees. *Drug Metab Dispos* **27:**1434–1447.
Rousu T, Pelkonen O, and Tolonen A (2009) Rapid detection and characterization of reactive drug metabolites in vitro using several isotope-labeled trapping agents and ultra-performance liquid chromatography/time-of-flight mass spectrometry. *Rapid Commun Mass Spectrom* **23:**843–855.
Scholz K, Dekant W, Völkel W, and Pähler A (2005) Rapid detection and identification of N-acetyl-L-cysteine thioethers using constant neutral loss and theoretical multiple reaction monitoring combined with enhanced product-ion scans on a linear ion trap mass spectrometer. *J Am Soc Mass Spectrom* **16:**1976–1984.
Seutter-Berlage F, van Dorp HL, Kosse HG, and Henderson PT (1977) Urinary mercapturic acid excretion as a biological parameter of exposure to alkylating agents. *Int Arch Occup Environ Health* **39:**45–51.
Siegers CP, Loeser W, Gieselmann J, and Oltmanns D (1984) Biliary and renal excretion of paracetamol in man. *Pharmacology* **29:**301–303.
Srivastava A, Maggs JL, Pirmohamed M, Park BK, and Williams DP (2008) Metabolic activation of nevirapine in human and rat systems. *Br J Clin Pharmacol* **65:**1001–1002.
Srivastava A, Williams DP, Maggs JL, Lian LY, Gardner I, Chaponda M, Pirmohamed M, Park BK, and Williams DP (2009) Bioactivation of nevirapine: characterization and quantification of nevirapine mercapturate in human urine. *Br J Clin Pharmacol*, **68:**276–277.
Stehbens WE (2004) Oxidative stress in viral hepatitis and AIDS. *Exp Mol Pathol* **77:**121–132.
Takakusa H, Masumoto H, Yukinaga H, Makino C, Nakayama S, Okazaki O, and Sudo K (2008) Covalent binding and tissue distribution/retention assessment of drugs associated with idiosyncratic drug toxicity. *Drug Metab Dispos* **36:**1770–1779.
Thompson CD, Barthen MT, Hopper DW, Miller TA, Quigg M, Hudspeth C, Montouris G, Marsh L, Perhach JL, Sofia RD, et al. (1999) Quantification in patient urine samples of felbamate and three metabolites: acid carbamate and two mercapturic acids. *Epilepsia* **40:**769–776.
Tsuruda LS, Lamé MW, and Jones AD (1995) Metabolism of [^{14}C]naphthalene in the B6C3F1 murine isolated perfused liver. *Drug Metab Dispos* **23:**129–136.
Uetrecht J (2003) Screening for the potential of a drug candidate to cause idiosyncratic drug reactions. *Drug Discov Today* **8:**832–837.
Veronese ME, McLean S, D'Souza CA, and Davies NW (1985) Formation of reactive metabolites of phenacetin in humans and rats. *Xenobiotica* **15:**929–940.
Walubo A, Barr S, and Abraham AM (2006) Rat CYP3A and CYP2B1/2 were not associated with nevirapine-induced hepatotoxicity. *Methods Find Exp Clin Pharmacol* **28:**423–431.
Wang Y, Zhong D, Chen X, and Zheng J (2009) Identification of quinone methide metabolites of dauricine in human liver microsomes and in rat bile. *Chem Res Toxicol* **22:**824–834.
Wen B, Chen Y, and Fitch WL (2009) Metabolic activation of nevirapine in human liver microsomes: dehydrogenation and inactivation of cytochrome P450 3A4. *Drug Metab Dispos* **37:**1557–1562.

Address correspondence to: D. P. Williams, MRC Centre for Drug Safety Science, Department of Pharmacology and Therapeutics, School of Biomedical Sciences, The University of Liverpool, Sherrington Buildings, Ashton Street, Liverpool L69 3GE, UK. E-mail: dom@liv.ac.uk